

# Use of a Fluorescence Spectroscopic Readout To Characterize the Interactions of Cdc42Hs with Its Target/Effector, mPAK-3<sup>†</sup>

David A. Leonard, Rohit S. Satoskar, Wen-Jin Wu, Shubha Bagrodia, Richard A. Cerione, and Danny Manor\*

Department of Pharmacology, Cornell University, Ithaca, New York 14853

Received September 10, 1996; Revised Manuscript Received November 25, 1996<sup>⊗</sup>

**ABSTRACT:** The family of p21-activated kinases (PAKs) has been shown to contain a domain that can independently bind to the Ras-like proteins Cdc42Hs and Rac. We have expressed a 72 amino acid recombinant form of this p21-binding domain (PBD) from mPAK-3 in *Escherichia Coli* for use in structure–function studies. The protein can be purified on a nickel affinity resin due to a hexa-His tag that is incorporated onto the amino terminus of the domain. PBD binds to Cdc42Hs in a guanine nucleotide-dependent manner as demonstrated by a novel fluorescence assay that takes advantage of the spectroscopic properties of *N*-methylanthraniloyl (Mant)-guanine nucleotides. Ionic strength has little effect on the affinity of PBD for Cdc42Hs, but alkaline pH values tend to weaken the interaction. We have shown that the inhibition of the GTPase activity of Cdc42Hs, as well as a previously undescribed inhibition of guanine nucleotide dissociation, is mediated by the PBD portion of the mPAK-3 molecule. These findings suggest that PBD binding alters the geometry of the guanine nucleotide binding site on Cdc42Hs, perhaps as an outcome of the target/effector molecule binding in close proximity to the nucleotide domain. We therefore tested if mutations in the effector region of Cdc42Hs (32–40), which in Ras are very close to the guanine nucleotide binding site, had any effect on PBD binding. Changing tyrosine 32 to lysine (Y32K) resulted in a small (5-fold) inhibition of PBD binding, but the very conservative mutation D38E yielded at least a 50-fold decrease in affinity. Finally, the catalytic domain of the GTPase activating protein, Cdc42-GAP, was shown to inhibit PBD binding in a competitive manner, indicating that this target molecule and the negative regulator (GAP) bind to overlapping sites on the Cdc42Hs molecule.

The Ras-superfamily of low molecular mass GTP-binding proteins plays essential roles in a variety of biological pathways including those that mediate cell-cycle progression, cytoskeletal alterations that stimulate cell shape changes and cell motility, and intracellular trafficking and secretion (Hall, 1990). The Ras-subfamily has been especially well studied because of the involvement of the Ras proteins in cell growth, differentiation, and possibly apoptosis. However, recently members of the Rho-subfamily, which include Cdc42Hs, Rac1, and RhoA, have also been receiving a significant amount of attention because of the suggestions that these GTP-binding proteins may work closely with Ras to provide a full complement of cell growth regulatory events (Qiu et al., 1995).

There are now a number of lines of evidence which indicate that Rho-subfamily proteins are essential for the normal regulation of cell growth and cytokinesis. These include the findings that Dbl (Hart et al., 1991; Cerione & Zheng, 1996) and a number of related oncoproteins [e.g., Ost, Lbc (Horii et al., 1994; Zheng et al., 1995)] or growth regulatory proteins [Tiam-1 (Michiels et al., 1995)] have been shown to catalyze the GDP–GTP exchange activities (and thus the activation of) Rho-subfamily proteins. In addition, a variety of growth regulatory proteins share sequence similarity with the Cdc42Hs-GTPase-activating protein (GAP), including Bcr, which has been implicated in the development of human leukemias (Diekmann et al., 1991), p190, which

binds to the Ras-GAP (Settleman et al., 1992), and 3BP-1, which was initially discovered through its ability to bind to the SH3 domain of the Abl tyrosine kinase (Cicchetti et al., 1995).

The most recent evidence for the involvement of Rho-subfamily proteins in the regulation of cell growth comes from the findings that Cdc42Hs and Rac1 stimulate the p70S6 kinase (Chou & Blenis, 1996) and the nuclear MAP kinases, the c-Jun kinase (JNK1) and p38 (Bagrodia et al., 1995a; Coso et al., 1995; Minden et al., 1995). The ability of Cdc42Hs and Rac1 to activate these nuclear MAP kinases appears to be the outcome of an interaction between the GTP-binding proteins and members of the family of p21-activated serine/threonine kinases (PAKs; Manser et al., 1994; Martin et al., 1995; Bagrodia et al., 1995a). Thus, Cdc42Hs and Rac appear to be capable of initiating a signaling pathway that leads to the nucleus and is analogous to the Ras signaling pathway that begins with the Raf serine/threonine kinase and culminates in the activation of the nuclear MAP kinases, the Erks [e.g., see Buday and Downward (1993)]. However, there are likely to be some interesting differences regarding the interactions of Cdc42Hs or Rac with members of the PAK family versus the interaction of Ras with Raf. For example, the principle role of Ras appears to be to recruit Raf to the membrane, where it then becomes activated through a mechanism that has yet to be determined. On the other hand, Cdc42Hs and/or Rac are absolutely essential for the stimulation of PAK activity; in the absence of these GTP-binding proteins, the PAKs show virtually no protein kinase activity.

<sup>†</sup> Supported by National Institutes of Health Grants GM47458 and EY06429.

\* Corresponding author.

<sup>⊗</sup> Abstract published in *Advance ACS Abstracts*, January 15, 1997.

In the present study, we have set out to develop methods for clearly defining the nature of the regulatory interaction between activated Cdc42Hs and mPAK-3, a ubiquitously distributed isoform of the PAK family (Bagrodia et al., 1995b). Toward this end, we have established an easy and highly-sensitive fluorescent readout for Cdc42Hs–mPAK-3 interactions that takes advantage of the fluorescent properties of the GTP analog *N*-methylantraniloyl GMP-PNP (Mant-GMP-PNP). Using this real-time assay, we have shown that a region of ~60 amino acids (designated PBD) contains all the necessary determinants for the high-affinity binding of GTP-bound Cdc42Hs to mPAK-3. We also have obtained direct evidence for the ability of PBD to inhibit both the [ $\gamma$ - $^{32}$ P]GTP hydrolytic activity of Cdc42Hs and [ $^{35}$ S]GTP $\gamma$ S dissociation and have used the fluorescence assay for PBD binding to show that the Cdc42Hs-GAP competes with the PBD for a common binding domain on the GTP-binding protein.

## MATERIALS AND METHODS

**Proteins.** The construction of a bacterial expression vector containing the DNA fragment encoding the p21-binding domain (PBD) of mPAK-3, fused to the glutathione *S*-transferase gene, has been described earlier (Bagrodia et al., 1995b). To achieve higher expression levels, this fragment was transferred into the *Bam*HI site of a modified pET15b vector, in-frame with the upstream hexa-histidine tag, and expressed in *E. coli* BL21(DE3).

Bacteria were grown in 4 L fermentors as described previously (Leonard et al., 1994). The bacterial pellet was thawed and homogenized in 100 mL of a lysis buffer (20 mM Tris-HCl, pH 8.0, 5 mM imidazole, 500 mM NaCl, 1 mM Na<sub>2</sub>S<sub>2</sub>O<sub>8</sub>, 200  $\mu$ M PMSF, 2  $\mu$ g/mL aprotinin, and 2  $\mu$ g/mL leupeptin), and lysozyme (Sigma) was added to 0.5 mg/mL. Upon completion of the lysis, 1 mg of DNase I (Boehringer) and 1 mL MgCl<sub>2</sub> (1 M) were added, and the suspension and incubated at 4 °C until no longer viscous (ca. 30 min). Following centrifugation (20 min, 10000g), the supernatant was applied to a 15 mL iminodiacetic acid–agarose column (Sigma) charged with Ni<sup>2+</sup>. The column was washed with TEDA buffer (20 mM Tris-HCl, pH 8.0, 5 mM imidazole, 500 mM NaCl, and 1 mM Na<sub>2</sub>S<sub>2</sub>O<sub>8</sub>) and further developed with a gradient of 5–200 mM imidazole, and 4 mL fractions were screened by SDS–PAGE. PBD-containing fractions (~80% pure) were pooled, brought to 55% saturation with ammonium sulfate, and resuspended in ~10 mL of TEDA buffer. The 17 amino acid hexa-His tag was removed by 2 h incubation (2 h) with 100  $\mu$ g of thrombin at 4 °C, and resolved by Q-Sepharose ion-exchange chromatography. Fractions containing PBD were pooled, precipitated with ammonium sulfate, dialyzed twice against TEDA buffer containing 40% glycerol, and stored at –20 °C.

Wild-type and mutated Cdc42Hs proteins were expressed in *E. coli* as hexa-histidine fusion proteins using pET15b and purified as described above for PBD [see also Leonard et al. (1994)]. Cloning of the carboxy-terminal catalytic domain of Cdc42Hs-GAP (residues 229–462; denoted here as GAP<sup>234</sup>) into a glutathione expression vector was described earlier (Barford et al., 1993). *E. coli* cells were grown, induced, and lysed as described above for Cdc42Hs. The GST-fusion protein was cleaved using thrombin (0.25 mg,

12 h, 4 °C), and then loaded onto a Q-Sepharose column (2.5  $\times$  10 cm) equilibrated with TEDA buffer. The column was developed with a linear NaCl gradient (0–300 mM); the pooled GAP<sup>234</sup> fractions (>95% pure by SDS–PAGE) were concentrated, dialyzed into buffer TEDA supplemented with 40% glycerol, and stored at –20 °C.

**Preparation of Mant-Nucleotides and Cdc42Hs/Mant-Nucleotide Complexes.** Mant-nucleotides were prepared as described earlier (Hiratsuka, 1983). Cdc42Hs was incubated with a 20-fold excess of purified Mant-nucleotide in the presence of 25 mM EDTA in TEDA buffer for 1.5 h at room temperature. MgCl<sub>2</sub> was added to a final concentration of 35 mM, and the mixture was filtered on a G-25 column (0.75  $\times$  45 cm) equilibrated with 20 mM Hepes–NaOH, pH 8.0, 5 mM MgCl<sub>2</sub>, and 1 mM sodium azide, (HMA buffer) to remove unbound nucleotides. The protein was then concentrated and dialyzed against HMA buffer supplemented with 40% glycerol and stored at –20 °C. Protein concentrations were determined by BCA assay (Pierce), and nucleotide concentrations were determined using published extinction coefficients (Hiratsuka, 1983).

**Fluorescence Measurements.** All measurements were done on an SLM 8000C spectrofluorometer [see Leonard et al. (1994)]. For Mant-nucleotides, excitation was set at 360 nm and the emission at 440 nm, using optical slit widths of 16 nm. All measurements were done at 25 °C with continual stirring in 20 mM Hepes–NaOH, pH 7.5, 5 mM MgCl<sub>2</sub>, and 100 mM NaCl unless otherwise indicated. For determination of the effects of ionic strength and pH on binding affinity, the buffer was modified to contain 0, 100, and 500 mM NaCl at pH 7.5, or the pH was set at the indicated value in 20 mM MES–NaOH (pH 5.5 and 6.5), Tris-HCl (7.5 and 8.5), or sodium borate (9.5) with a constant salt concentration of 100 mM.

**Data Analysis.** Fluorescence titration data (such as shown in Figures 3, 6, and 7 and Table 1) were fit to a simple bimolecular association model. The association between Cdc42Hs (C) and an effector (E)



can be described by a simple bimolecular interaction equation:

$$[CE] = \frac{[E]_T[C]}{[C] + K_d} \quad (2)$$

where [CE] is the concentration of the formed complex at equilibrium, [C] is the concentration of free Cdc42Hs in solution, [E]<sub>T</sub> is the total effector concentration, and *K*<sub>d</sub> is the equilibrium dissociation constant. Since in this experimental system it cannot be assumed that only a small, negligible fraction of the total Cdc42Hs is bound, and because the concentration of free Cdc42Hs is not easily measured, it is necessary to fit the data to the quadratic form of the solution. Thus, fluorescence titration data were fit to the expression:

$$F = \frac{-K_d + E_T + C_T + \sqrt{(K_d + E_T + C_T)^2 - 4C_TE_T}}{2C_T} (F_i - F_0) + F_0 \quad (3)$$

where  $F$  is the fluorescence intensity,  $E_T$  is total effector concentration at any point in the titration, and  $F_0$  and  $F_f$  are the fluorescence intensities at the starting point and end point of the titration, respectively. Fitting of the data was done using a commercially available data analysis for Macintosh (Igor, WaveMetrics Inc., Lake Oswego, OR).

**GTPase Assays.** The GTP hydrolytic activity of Cdc42Hs was measured by assaying the release of [ $^{32}$ P]P<sub>i</sub> from [ $\gamma$ - $^{32}$ P]GTP bound to the protein. First, Cdc42Hs (10  $\mu$ M) was incubated with 7  $\mu$ M [ $\gamma$ - $^{32}$ P]GTP (360 000 cpm/pmol) in 20 mM Tris-HCl, pH 7.5, 10 mM EDTA, 1 mM DTT, 50 mM NaCl, and 80  $\mu$ g/mL bovine serum albumin, for 20 min at room temperature. To initiate hydrolysis of the bound GTP, aliquots of the Cdc42Hs were then diluted into a reaction mixture containing 25 mM Tris-HCl, pH 7.5, 1.3 mM DTT, 40 mM NaCl, 5 mM MgCl<sub>2</sub>, 200  $\mu$ g/mL bovine serum albumin, 100  $\mu$ M nonradioactive GTP, and either purified PBD or control buffer (TEDA buffer, 40% glycerol). Aliquots were removed at the indicated times and filtered on BA-85 nitrocellulose filters (Schleicher & Schuell), and the amount of  $^{32}$ P still associated with Cdc42Hs was determined by liquid scintillation counting of the filters. The concentration–response curve was generated by the same method except that different dilutions of purified PBD were used as indicated, and all samples were filtered following 20 min in the hydrolysis reaction.

**Nucleotide Exchange.** Complexes of Cdc42Hs with radioactive nucleotide were as described above except that 10  $\mu$ M [ $^{35}$ S]GTP $\gamma$ S (specific activity 31 000 cpm/pmol) was used instead of [ $\gamma$ - $^{32}$ P]GTP. After 30 min at room temperature, Cdc42Hs was diluted into a reaction mixture containing 25 mM Tris-HCl, pH 7.5, 1.3 mM DTT, 40 mM NaCl, 2.5 mM EDTA, 200  $\mu$ g/mL bovine serum albumin, 0.5 mM nonradioactive GTP $\gamma$ S, and either 10.6  $\mu$ M PBD or control buffer. Aliquots were removed at the indicated time points and filtered on nitrocellulose to determine the fraction of bound [ $^{35}$ S]GTP $\gamma$ S. The concentration–response curve was generated by using different amounts of PBD and filtering after 40 min of dissociation.

Dissociation and hydrolysis kinetic data were fit to a single exponential function, and the concentration–response curves were fit to a model for a bimolecular reaction as described above.

## RESULTS

**Expression of the p21-Binding Domain (PBD) of mPAK-3.** Sequence alignments of different members of the PAK family of serine/threonine kinases have shown that a stretch of ~60 amino acids is likely to contain the main binding determinants for Cdc42Hs and Rac (Burbelo et al., 1995). This region, originally termed PBD (p21-binding domain) and later CRIB (Cdc42Hs and Rac interactive-binding domain), appears to be present in a number of putative targets for Cdc42Hs and Rac including the activated-Cdc42Hs (tyrosine) kinase (ACK; Manser et al., 1993), the Wiscott–Aldrich Syndrome protein (WASP; Aspenstrom et al., 1996), and the p70S6 kinase (Chou & Blenis, 1996). In order to fully characterize the biochemical properties of such domains, we have recloned the PBD domain (residues 65–137) from mPAK-3 (Bagrodia et al., 1995b) into the bacterial expression vector pET-15b and expressed it as a hexa-histidine-tagged protein. The protein was purified using Ni<sup>2+</sup> affinity chromatography, ammonium sulfate precipitation, and ion

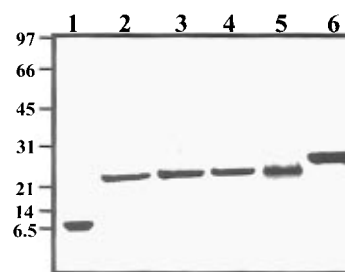


FIGURE 1: SDS–PAGE profiles for the purified, recombinant proteins used in this study. Protein samples (7  $\mu$ g) were boiled in Laemmli buffer, resolved on 14% acrylamide gels, and visualized by Coomassie Blue staining. Lane 1, PBD; lane 2, D38E Cdc42Hs; lane 3, Y32K Cdc42Hs; lane 4, Q61L Cdc42Hs; lane 5, Cdc42Hs; lane 6, GAP<sup>234</sup>.

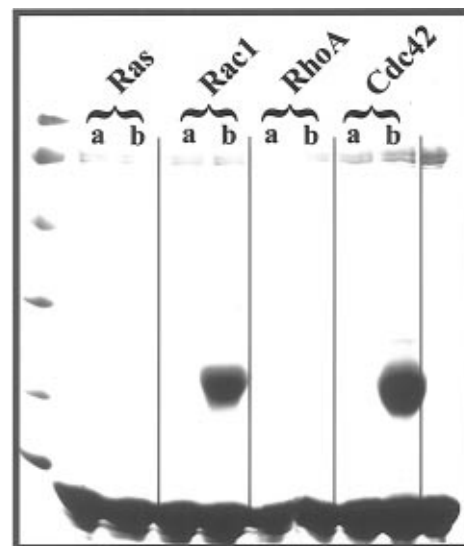


FIGURE 2: Binding of low molecular weight GTPases using hexa-histidine-tagged PBD. The various GTPases were complexed with the indicated nucleotide using EDTA as described under Materials and Methods, and filtered on Pharmacia PD-10 columns equilibrated with HMA buffer. The purified proteins (80  $\mu$ g) were incubated with 15  $\mu$ L of iminodiacetic acid–agarose beads and PBD (20  $\mu$ g) in 20 mM Tris-HCl, pH 8.0, 5 mM imidazole, 500 mM NaCl, and 1 mM NaN<sub>3</sub> for 30 min at 4 °C. Following five centrifugation washes in the same buffer, 20  $\mu$ L of each reaction was resolved on 12% SDS–PAGE and visualized using Coomassie blue staining. a, GDP complexes; b, GTP $\gamma$ S.

exchange chromatography to >95% purity (see Materials and Methods). Figure 1 shows the SDS–PAGE analysis of the recombinant purified PBD (lane 1) and the individual GTP-binding proteins examined in this study (lanes 2–6).

**Recombinant PBD Is Able To Specifically Interact with Cdc42Hs.** We have used the recombinant histidine-tagged PBD domain as an affinity reagent to examine the specificity of the PBD for RhoA, Rac1, and Cdc42Hs in their GDP-bound and GTP $\gamma$ S-bound states. Following incubation with the respective GTP-binding protein and extensive washes, the immobilized PBD was subjected to SDS–PAGE and visualized by Coomassie Blue staining (see Figure 2). The data in Figure 2 clearly show that the PBD binds with high specificity to the GTP $\gamma$ S-bound forms of Cdc42Hs and Rac. The PBD did not show detectable binding to RhoA or Ras, nor to the GDP-bound states of Cdc42Hs or Rac. Thus, the specificity that has been observed for Cdc42Hs and Rac interactions with the full-length mPAK-3 molecule (Bagrodia et al., 1995b; Manser et al., 1994b) is fully preserved within the PBD.

**Development of a Fluorescence Readout for the Binding of PBD to Cdc42Hs.** In order to obtain quantitative information regarding the binding of PBD to Cdc42Hs, we developed a real-time fluorescence spectroscopic assay to monitor this protein–protein interaction. The assay is based on the fluorescent properties of *N*-isotoic- (Mant-) modified guanine nucleotides which we (Leonard et al., 1994) and others (Rensland et al., 1991; Moore et al., 1993) have shown to serve as sensitive reporter groups for the immediate environment of the nucleotide-binding site on Cdc42Hs and related GTP-binding proteins. Cdc42Hs can be complexed with Mant-derivatized guanine nucleotides by reducing the  $Mg^{2+}$  concentration with excess EDTA, such that the GDP that was originally bound to Cdc42Hs is dissociated and replaced by the Mant-nucleotide (e.g., Mant-GMP-PNP). The excess (unbound) Mant-GMP-PNP is then removed by gel filtration chromatography, yielding a Cdc42Hs molecule that is labeled stoichiometrically (1:1) with Mant-GMP-PNP.

Figure 3 shows the results obtained when the recombinant PBD was added to the Cdc42Hs–Mant-GMP-PNP complex. The addition of the PBD yielded a dose-dependent increase in the Mant emission intensity (excitation 360 nm, Figure 3A). The increased fluorescence was not accompanied by a detectable shift in the wavelength of the maximum emission, which suggests that the PBD does not significantly alter the hydrophobic nature of the immediate environment of the Mant fluorophore. Rather, it is more likely that the binding of the PBD reduces the accessibility of the Mant moiety to an amino acid side chain which quenches its fluorescence (i.e., as an outcome of a PBD-induced conformational change within the Cdc42Hs molecule).

Figure 3B shows the time course for the PBD-induced change in Mant fluorescence (for Mant-GMP-PNP bound to Cdc42Hs) at constant excitation (360 nm) and emission (440 nm) wavelengths. The PBD caused an  $\sim 2$ -fold enhancement of the Mant fluorescence that was complete within the time period of mixing ( $< 3$  s). The addition of the GTPase-defective Cdc42Hs mutant (Cdc42Hs[Q61I]), which is purified with tightly bound GTP, fully reversed the PBD-induced enhancement of the Mant fluorescence, whereas the addition of wild-type GDP-bound Cdc42Hs had very little effect. Thus, the binding of the PBD to Cdc42Hs, as monitored by changes in the Mant-GMP-PNP fluorescence, is fully reversible and shows the same specificity for the nucleotide state of Cdc42Hs that was originally observed in affinity precipitation experiments using His-PBD (Figure 2).

Figure 4 shows a binding isotherm that was obtained when monitoring the PBD-induced changes in Mant-GMP-PNP bound to Cdc42Hs. The titration data could be fit to a simple bimolecular equilibrium model (see Materials and Methods) and yielded an apparent  $K_d$  value of  $0.9 \mu M$  for the interaction of PBD with Cdc42Hs–Mant-GMP-PNP. When a similar titration was performed with the Cdc42Hs–Mant-GDP species, a relatively weak but detectable enhancement of the Mant fluorescence was observed. If we assume an identical fluorescence end point (as observed with Mant-GMP-PNP), the fitting of the fluorescence data yielded a lower limit  $K_d$  value of  $\sim 70 \mu M$  for the binding of PBD to the Cdc42Hs–Mant-GDP complex. This then suggests that the PBD binds to the Mant-GDP-bound Cdc42Hs with an at least  $\sim 70$ -fold weaker affinity compared to its binding to the Cdc42Hs–Mant-GMP-PNP species.

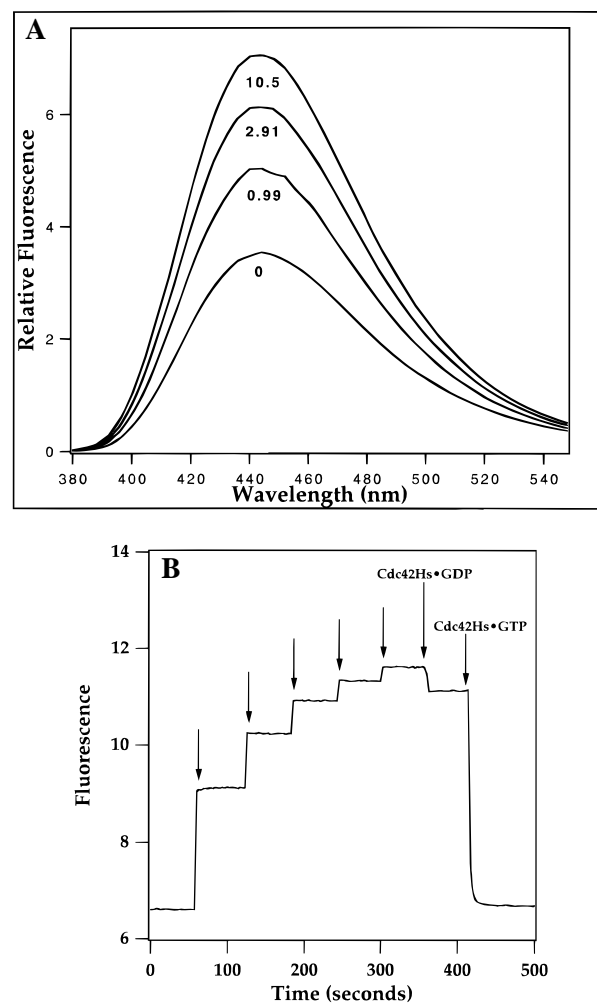


**FIGURE 3:** Fluorescence assay for the interaction of Cdc42Hs–Mant-GMP-PNP with PBD. (A) One micromolar Cdc42Hs–Mant-GMP-PNP was incubated in HMN buffer, and its emission spectrum was measured (excitation, 360 nm; emission resolution, 4 nm, 25 °C). PBD was then added to the final concentrations indicated (in  $\mu M$ ), and emission spectra were obtained. Each spectrum is an average of two scans. (B) One micromolar Cdc42Hs–Mant-GMP-PNP was added to the fluorescence cuvette, and the Mant fluorescence (emission, 440 nm; excitation, 360 nm) was monitored. At the times indicated by the arrows, PBD was added to final concentrations of 0.98, 1.97, 2.95, 3.92, and  $4.90 \mu M$ . To assess the reversibility and selectivity of the PBD–Cdc42Hs–Mant-GMP-PNP interaction, wild-type (GDP-bound) Cdc42Hs and the Cdc42Hs(Q61I) mutant (GTP-bound) were added at the indicated times to final concentrations of 40 and  $29 \mu M$ , respectively.

Since we are interested in obtaining structural information regarding a Cdc42Hs–PBD complex, we assayed the binding of PBD to Mant-GMP-PNP-bound Cdc42Hs under a number of different conditions. Table 1 shows the  $K_d$  values for the PBD–Cdc42Hs interaction measured at different concentrations of NaCl and at different pH values. We found that NaCl concentrations between 0 and 500 mM had only subtle effects on the binding affinity, with the  $K_d$  values ranging from 0.9 to  $1.7 \mu M$ . However, when the pH of the incubation was varied, we observed a marked weakening of the interaction (nearing a 50-fold increase in the dissociation constant) at pH 9.5, while optimal binding between PBD and Cdc42Hs occurred at pH 6.5.

**PBD Acts as an Inhibitor of GTP Hydrolysis and Guanine Nucleotide Exchange.** During the initial identification of PAK as a Rac1/Cdc42Hs target, it was shown that PAK inhibited both intrinsic and GAP-accelerated

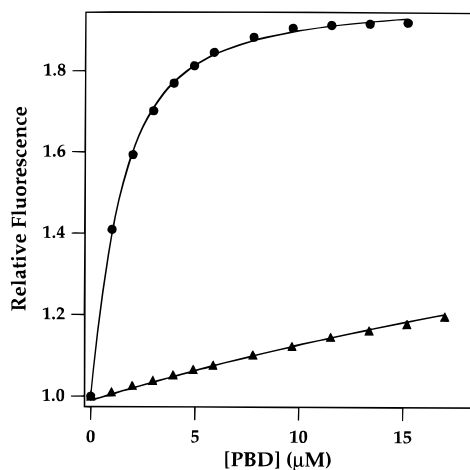


FIGURE 4: Fluorescence titration of Cdc42Hs•Mant-GMP-PNP with PBD. Experimental conditions were as described in Figure 3. One micromolar of either Cdc42Hs•Mant-GMP-PNP (circles) or Cdc42Hs•Mant-GDP (triangles) was titrated with the indicated amounts of PBD, while monitoring Mant fluorescence. Solid lines represent fits of the data to a bimolecular association model as described under Materials and Methods.

Table 1: Effects of pH and Ionic Strength on the Association of PBD with Cdc42Hs•mGMP-PNP<sup>a</sup>

pH	[NaCl] (mM)	$K_d$ ( $\mu$ M)
5.5	100	0.47
6.5	100	0.38
7.5	100	1.3
8.5	100	7.5
9.5	100	17.0
7.5	0	1.7
7.5	100	0.92
7.5	500	1.2

<sup>a</sup> A fluorescence binding titration (12 PBD concentrations between 0 and 30  $\mu$ M) was performed at each condition and the dissociation constant derived as described in Figure 3.

hydrolysis of GTP by the Rac1 protein (Manser et al., 1994). We investigated whether the PBD was sufficient to elicit this GTPase-inhibitory effect. Cdc42Hs was first complexed with [ $\gamma$ -<sup>32</sup>P]GTP in the presence of EDTA. MgCl<sub>2</sub> was then added to initiate hydrolysis, in the presence of either control buffer or purified PBD, and aliquots were filtered on nitrocellulose at the time intervals indicated in Figure 5A. It can be seen that in the absence of any added PBD, Cdc42Hs hydrolyzed GTP rapidly (i.e., the half-time for the reaction was 3–4 min at room temperature). However, in the presence of 10  $\mu$ M PBD, a significant decrease in the rate of <sup>32</sup>P release from the GTPase was observed ( $t_{1/2}$  = 17 min).

Figure 5B shows that the GTPase inhibitory activity is dependent on the PBD concentration. It is interesting that even at concentrations of PBD significantly below (e.g., 50 nM) the level used in the fluorescence binding assay described above (see Figure 4A), a complete inhibition of GTP hydrolysis was observed. When the dose–response data shown in Figure 5B were fitted to an association reaction, a  $K_d$  value of 27 nM was obtained, which suggested a significantly tighter interaction between the PBD and GTP-bound Cdc42Hs, compared to that measured for PBD and Mant-GMP-PNP-bound Cdc42Hs. Similar experiments utilizing Cdc42Hs bound to Mant-GTP instead of the nonhydrolyzable GMP-PNP yield similar  $K_d$  values (T. Nomanbhoy and R. Cerione, in preparation). This strongly suggests that the Mant modification of the guanine nucleotide influences

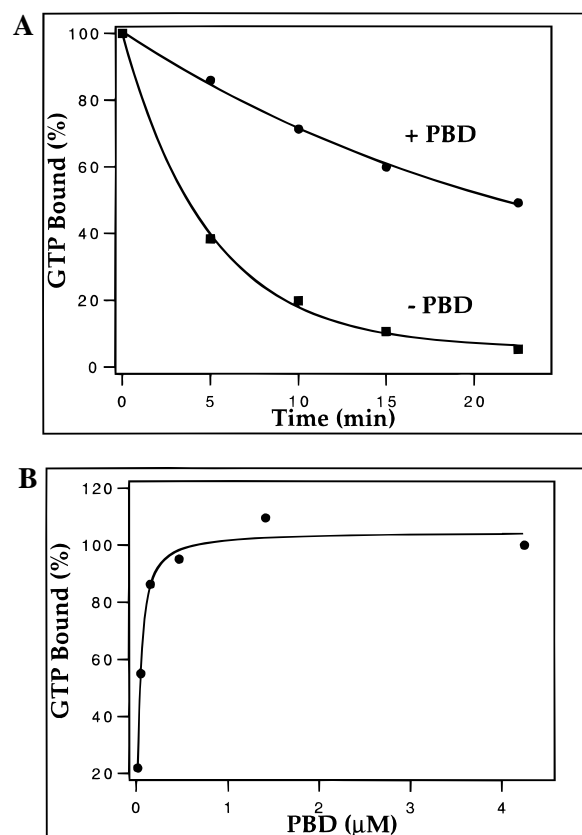


FIGURE 5: Inhibition of the GTPase activity of Cdc42Hs by PBD. (A) Time course for the amount of [ $\gamma$ -<sup>32</sup>P]GTP associated with Cdc42Hs following Mg<sup>2+</sup>-induced GTP hydrolysis in the presence or absence of 10.6  $\mu$ M PBD. Solid lines represent a fit to a single exponential process ( $t_{1/2}$  = 17.0 and 3.4 min in the presence and absence of PBD, respectively). (B) Dose–response curve for the inhibition of GTPase activity. Indicated amounts of PBD were added to a GTPase reaction assay (see above and Materials and Methods), and the amount of protein-associated radioactivity was measured after 20 min. The solid line represents the best fit of the data to a bimolecular association model as described under Materials and Methods.

the affinity of the binding of Cdc42Hs to PBD (see Discussion).

We next investigated whether PBD had any effect on the rate of guanine nucleotide exchange from Cdc42Hs. First, [<sup>35</sup>S]GTP $\gamma$ S was exchanged onto Cdc42Hs in the presence of EDTA. The dissociation of the radiolabeled GTP $\gamma$ S was then initiated by the addition of excess unlabeled GTP $\gamma$ S, in the presence or absence of PBD. Figure 6A shows the amount of radiolabeled nucleotide still bound to Cdc42Hs at the indicated time points, as detected by nitrocellulose filter-binding assay. In the absence of PBD, GTP $\gamma$ S dissociation from Cdc42Hs was rapid with a  $t_{1/2}$  of ~10 min. However, in the presence of the PBD, GTP $\gamma$ S dissociation from Cdc42Hs was completely eliminated. The concentration–response curve shown in Figure 5B indicates that the apparent  $K_d$  for the interaction between PBD and Cdc42Hs (which leads to the inhibition of GTP $\gamma$ S dissociation) is ~30 nM, which again is significantly tighter than that measured for the binding of PBD to Mant-GMP-PNP-bound Cdc42Hs.

**Binding of PBD to Cdc42Hs Effector Region Mutants.** Given the ability of the PBD to cause significant perturbations to the hydrolysis and binding of guanine nucleotides by Cdc42Hs, and its ability to elicit changes in the fluorescence of (bound) Mant-guanine nucleotides, we

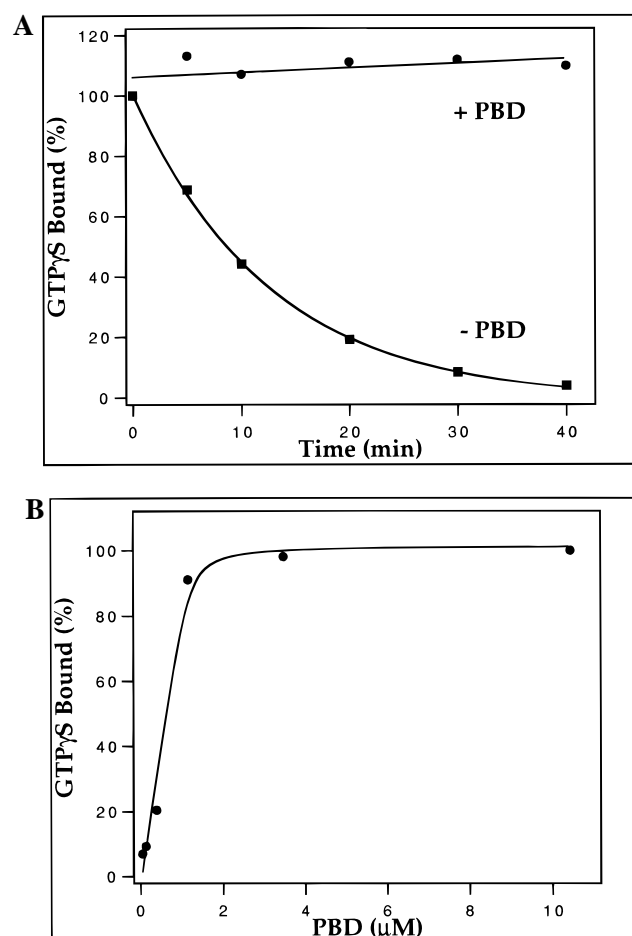


FIGURE 6: Inhibition of guanine nucleotide dissociation from Cdc42Hs by PBD. (A) Time-course for the amount of  $[^{35}\text{S}]\text{GTP}\gamma\text{S}$  associated with Cdc42Hs following EDTA-induced guanine nucleotide dissociation in the presence and absence of 10.6  $\mu\text{M}$  PBD. Solid lines represent a fit to a single exponential process in the absence of PBD ( $t_{1/2} = 8.6$  min), and to a linear function in the presence of PBD. (B) Dose-response curve for the inhibition of guanine nucleotide exchange. Indicated amounts of PBD were added to a  $[^{35}\text{S}]\text{GTP}\gamma\text{S}$  dissociation assay (see above and Materials and Methods), and the amount of protein-associated radioactivity was measured after 40 min. The solid line represents the fit of the data to the bimolecular association model as described under Materials and Methods.

reasoned that the PBD may bind closely to the guanine nucleotide itself. Also, because the PBD can discriminate between the GDP- and GTP-bound forms of Cdc42Hs, a likely binding site would be the so-called switch I effector loop which has been shown to contribute to the binding interface between Ras and the Raf kinase (Nassar et al., 1995) as well as between Rac and its GAP (Diekman et al., 1995; Lamarche et al., 1996). In order to examine the latter possibility, two mutant Cdc42Hs proteins were expressed in *E. coli*. One mutant contained a lysine in place of the normal tyrosine at position 32 [i.e., Cdc42Hs(Y32K)], while in the second mutant, a glutamic acid residue was substituted for aspartic acid at position 38 [Cdc42Hs(D38E)]. The latter was shown to be a key residue for the GTP-specific interaction of the Rap and Ras GTP-binding proteins with a limit domain on the Raf kinase; in these cases, aspartic acid 38 appears to form a salt-bridge with a target basic residue (R89 in Raf). The Cdc42Hs mutants were precomplexed with Mant-GMP-PNP and titrated with PBD as described in Figure 3. The results presented in Figure 7 show that the

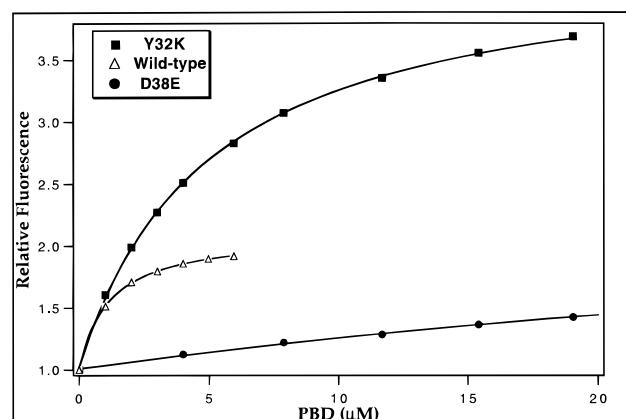


FIGURE 7: Association of PBD with effector mutants of Cdc42Hs. Titrations of protein-bound Mant-GMP-PNP were carried out as described in Figure 3, using the Cdc42Hs(D38E) mutant (circles), Cdc42Hs(Y32K) (squares), or wild-type Cdc42Hs (triangles). Each of the Cdc42Hs proteins showed identical levels of guanine nucleotide binding, nucleotide exchange, and GTP hydrolysis activities (data not shown). Solid lines represent the best fit of the data to a bimolecular association model as described under Materials and Methods.

Table 2: Competition between PBD and Cdc42-GAP on Binding to Cdc42Hs-mGMP-PNP<sup>a</sup>

[GAP] ( $\mu\text{M}$ )	initial fluorescence	final fluorescence	$K_d$ ( $\mu\text{M}$ )
0	1.005	2.06	1.1
2.5	1.01	2.01	2.7
5.5	1.003	2.06	4.5

<sup>a</sup> Titrations were carried out using Mant fluorescence as described in Figure 3, in the presence of the indicated amounts of Cdc42-GAP. Dissociation constant were extracted from fits of the data to the association reaction described under Materials and Methods.

PBD does bind to the Cdc42Hs(Y32K) mutant, albeit somewhat weaker than its binding to wild-type Cdc42Hs (i.e., there is an  $\sim 5$ -fold increase in the apparent  $K_d$ ). The Cdc42Hs(D38E) mutant, on the other hand, binds with a significantly lower affinity to the PBD (i.e., there is at least a 50-fold increase in the apparent  $K_d$  value). It is interesting that the extent of PBD-induced enhancement of the Mant fluorescence measured for the Cdc42Hs(Y32K) mutant differs significantly from that for the wild-type Cdc42Hs protein. Specifically, the binding of the PBD to Cdc42Hs-(Y32K) induces a 5-fold enhancement in the Mant fluorescence, compared to the 2-fold enhancement observed with the wild-type GTP-binding protein.

**Inhibition of PBD Binding with the Catalytic Domain of Cdc42HsGAP.** The observation that the interaction of PBD with Cdc42Hs is sensitive to mutations in the effector domain of Cdc42Hs, a region previously implicated in GAP binding, is suggestive of a common binding site (on Cdc42Hs) for the negative-regulator (GAP) and the target (PAK). We tested this directly by measuring the effects of increasing concentrations of the Cdc42Hs-GAP catalytic domain on the binding of the PBD to Cdc42Hs. The results of this competition experiment are presented in Table 2. We found that the presence of the Cdc42Hs-GAP increased the dissociation constant for the PBD-Cdc42Hs-binding interaction (as measured by PBD-induced changes in Mant-GMP-PNP fluorescence), without affecting the titration end point (i.e., the maximal level of fluorescence change that can be attained at saturating levels of the PBD). These results are consistent with there being a simple competition between

PBD and the Cdc42Hs-GAP for a common binding site on the Cdc42Hs molecule.

## DISCUSSION

During the past few years, a great deal of research attention has been directed toward the role of Rho-subfamily GTP-binding proteins in a variety of biological processes. It originally was felt that the primary roles for Rho, Rac, and Cdc42Hs involved the regulation of a defined set of cytoskeletal changes (Ridley & Hall, 1992; Ridley et al., 1992; Kozma et al., 1995; Nobes & Hall, 1995); however, more recently, it has become clear that these GTP-binding proteins may play an important part in the regulation of cell-cycle progression and cytokinesis. Related to this is the growing appreciation that each of these GTP-binding proteins are capable of stimulating multiple target/effector molecules. This has been especially highlighted for the case of Cdc42Hs, where it recently has been shown to engage a variety of putative targets including the 85 kDa regulatory subunit (p85) of the PI 3-kinase (Zheng et al., 1994), the Wiscott–Aldrich syndrome protein (WASP; Aspenstrom et al., 1996), the IQ-GAP molecules (Hart et al., 1996; McCallum et al., 1996), the p70S6 serine/threonine kinase (Chou & Blenis, 1996), the ACK tyrosine kinase (Manser et al., 1993), and members of the PAK family of serine/threonine kinases (Manser et al., 1994a; Bagrodia et al., 1995b). Although it is suspected that all of these potential Cdc42Hs-signaling responses may be coordinated, the biochemical details underlying most of these putative target interactions remain to be elucidated. However, a significant amount of information has been recently obtained for Cdc42Hs (or Rac1) interactions with the PAKs (Bagrodia et al., 1995a; Martin et al., 1995; Minden et al., 1995a; Coso et al., 1995; Zhang et al., 1995), such that the current thinking is that the stimulation of PAK activity by Cdc42Hs/Rac1 initiates a protein kinase cascade that leads to the nucleus and culminates in the activation of two nuclear (stress-activated) MAP kinases, JNK1 and p38. This is likely to be analogous to a pathway in *Saccharomyces cerevisiae*, where the PAK homolog Ste20 initiates a kinase cascade that results in the activation of the MAP kinase Fus3/Kss1 (Otilie et al., 1995).

In the original identification of the brain PAK (also designated mPAK-1) as a putative target for Cdc42Hs and Rac1, it was appreciated that a limited region of sequence homology was shared between the PAK molecule and ACK (Manser et al., 1994a). This region, originally designated the p21-binding domain (PBD) or the Cdc42/Rac-interactive-binding domain (CRIB), also appears to be present in WASP and p70S6 kinase and thus is likely to represent an important determinant in the binding of GTP-binding proteins (Burbelo et al., 1995). Studies with the full length PAK molecules have highlighted some important characteristics for their interactions with GTP-binding proteins; these include (i) PAK binding is specific for the Cdc42Hs and Rac1 proteins (and is not observed with RhoA, Ras, or any other members of the Ras superfamily), (ii) PAK binding is highly selective for the GTP-bound forms of Cdc42Hs and Rac1, and (iii) PAK binding appears to result in an inhibition of the GTPase activity of Cdc42Hs/Rac1. In the present study, we set out to determine whether these different characteristics were demonstrated by the PBD/CRIB domain of mPAK-3. Using a highly sensitive fluorescence assay that provides a specific signal for PBD binding to Cdc42Hs (i.e., an enhancement

of the fluorescence of bound Mant-GMP-PNP), we have found that the PBD is capable of all of the biochemical activities observed with full-length mPAK-3. Whether additional interactions occur between Cdc42Hs and the full-length PAK is not known at present. However, since we observe high-affinity binding to the PBD region of PAK, it is likely that any additional interactions, should they exist, are limited.

It is interesting that the binding of the PBD to Cdc42Hs results in a strong inhibition of guanine nucleotide dissociation. In fact, the inhibition of guanine nucleotide dissociation caused by the binding of the PBD is even more pronounced than that measured with the GDP dissociation inhibitor (GDI). Specifically, the PBD is able to completely inhibit the dissociation of GDP (see Figure 6A) under conditions where we routinely observed a 60% inhibition with the GDI. In addition, the PBD is also able to strongly inhibit GTP dissociation (as well as GDP dissociation) from Cdc42Hs (which is not the case for the GDI molecule). Moreover, PBD elicits its GDI activity on Cdc42Hs produced in *E. coli* (Figure 6) whereas Rho-GDI inhibits nucleotide dissociation only from posttranslationally modified Cdc42Hs (Leonard et al., 1992). These findings seem to indicate that the PBD is likely to bind in close proximity to the guanine nucleotide site on the Cdc42Hs molecule, whereas Rho-GDI requires interaction with the (isoprenylated) carboxy terminal of Cdc42Hs. This also is consistent with the fact that the PBD induces a strong enhancement in the fluorescence of Mant-GMP-PNP (bound to Cdc42Hs) and that PBD binding appears to be weakened by the presence of the Mant moiety. Some portion of the putative effector loop/‘switch-1’ domain (residues 32–42) on Cdc42Hs also is likely to be involved in binding the PAK molecules, since mutations within this region influence the binding affinity of PBD. The ability of the Cdc42Hs-GAP to compete with PBD for binding to Cdc42Hs supports the idea that PAK binds to a region within the ‘switch-1’ domain that is in close proximity to the guanine nucleotide site. It is worth noting that the binding site for PAK (as determined by its PBD) on Cdc42Hs appears to be overlapping but nonetheless distinct from the binding site for another class of targets, the IQ-GAP molecules (McCallum et al., 1996). An important area of future work will be to determine how different regulators and targets influence the binding of PBD to activated Cdc42Hs and ultimately the specific mechanism that underlies the conversion of this binding interaction into a marked stimulation of PAK activity.

## REFERENCES

- Aspenstrom, P., Lindberg, U., & Hall, A. (1996) *Curr. Biol.* 6(1), 70–75.
- Bagrodia, S., Derigard, B., Davis, R. J., & Cerione, R. A. (1995a) *J. Biol. Chem.* 270, 27995–27998.
- Bagrodia, S., Taylor, S., Creasy, C., Chernoff, J., & Cerione, R. (1995b) *J. Biol. Chem.* 270, 22731–22737.
- Barford, E. T., Zheng, Y., Kuang, W. J., Hart, M. J., Evans, T., Cerione, R. A., & Ashkenazi, A. (1993) *J. Biol. Chem.* 268(15), 26059–26062.
- Buday, L., & Downward, J. (1993) *Cell* 73, 611–620.
- Burbelo, P. D., Drechsel, D., & Hall, A. (1995) *J. Biol. Chem.* 270(49), 29071–29074.
- Cerione, R. A., & Zheng, Y. (1996) *Curr. Opin. Cell Biol.* 8(2), 205–215.
- Chou, M. M., & Blenis, J. (1996) *Cell* 85, 573–583.

- Cicchetti, P., Ridley, A. J., Zheng, Y., Cerione, R. A., & Baltimore, D. (1995) *EMBO J.* 14, 3127–3125.
- Coso, O., Chiariello, M., Yu, J. C., Teramoto, H., Crespo, P., Xu, N., Miki, T., & Gutkind, S. (1995) *Cell* 81, 1137–1146.
- Diekman, D., Nobes, C. D., Burbello, P. D., Abo, A., & Hall, A. (1995) *EMBO J.* 14(21), 5297–5305.
- Diekmann, D., Brill, S., Garret, M. D., Totty, N., Hsuan, J., Monfries, C., Hall, C., Lim, L., & Hall, A. (1991) *Nature* 351, 400–402.
- Hall, A. (1990) *Science* 249, 635–640.
- Hart, M., Callow, M., Souza, B., & Polakis, P. (1996) *EMBO J.* 15, 2997–3005.
- Hart, M. J., Eva, A., Evans, T., Aaronson, S. A., & Cerione, R. A. (1991) *Nature* 354, 311–314.
- Hiratsuka, T. (1983) *Biochim. Biophys. Acta* 742, 496–508.
- Horii, Y., Beeler, J. F., Sakaguchi, K., Tachibana, M., & Miki, T. (1994) *EMBO J.* 13, 4776–4786.
- Kozma, R., Ahmed, S., Best, A., & Lim, L. (1995) *Mol. Cell. Biol.* 15(4), 1942–1952.
- Lamarche, N., Tapon, N., Stowers, L., Burbello, P. D., Aspenström, P., Bridges, T., Chant, J., & Hall, A. (1996) *Cell* 87(3), 519–529.
- Leonard, D., Hart, M. J., Platko, J. V., Eva, A., Henzel, W., Evans, T., & Cerione, R. A. (1992) *J. Biol. Chem.* 267(32), 22860–22868.
- Leonard, D. A., Evans, T., Hart, M., Cerione, R. A., & Manor, D. (1994) *Biochemistry* 33, 12323–12328.
- Manser, E., Leung, T., Salihuddin, H., Tan, L., & Lim, L. (1993) *Nature* 363, 364–367.
- Manser, E., Leung, T., Salihuddin, H., Zhao, Z., & Lim, L. (1994) *Nature* 367, 40–46.
- Martin, G. A., Bollag, G., McCormick, F., & Abo, A. (1995) *EMBO J.* 14, 1970–1978.
- McCallum, S. J., Wu, W. J., & Cerione, R. A. (1996) *J. Biol. Chem.* (in press).
- Michiels, F., Habets, G. M. G., Stam, J. C., Van Der Kammer, R. A., & Collard, J. G. (1995) *Nature* 375, 338–340.
- Minden, A., Lin, A., Claret, F. X., Abo, A., & Karin, M. (1995) *Cell* 81, 1147–1157.
- Moore, K. J. M., Webb, M. R., & Eccleston, J. F. (1993) *Biochemistry* 32, 7451–7459.
- Nassar, N., Horn, G., Herrmann, C., Scherer, A., McCormick, F., & Wittinghofer, A. (1995) *Nature* 375, 554–560.
- Nobes, C. D., & Hall, A. (1995) *Cell* 81, 53–62.
- Ottillie, S., Miller, P., Johnson, D., Creasy, C., Sells, M. A., Bagrodia, S., Forsburg, S., & Chernoff, J. (1995) *EMBO J.* 14(23), 5908–5919.
- Qiu, R. G., Chen, J., Kim, D., McCormick, F., & Symons, M. (1995) *Nature* 374, 457–459.
- Rensland, H., Lautwein, A., Wittinghofer, A., & Goody, R. S. (1991) *Biochemistry* 30, 11181–11185.
- Ridley, A. J., & Hall, A. (1992) *Cell* 70, 389–399.
- Ridley, A. J., Paterson, H. F., Johnston, C. L., Diekmann, D., & Hall, A. (1992) *Cell* 70, 401–410.
- Settleman, J., Narasimhan, V., Foster, L. C., & Weinberg, R. A. (1992) *Cell* 69, 539–549.
- Zhang, S., Han, J., Sells, N. A., Chernoff, J., Knaus, U. G., Ulevitch, R. J., & Bokoch, G. M. (1995) *J. Biol. Chem.* 270, 23934–23936.
- Zheng, Y., Bagrodia, S., & Cerione, R. (1994) *J. Biol. Chem.* 269(29), 18727–18730.
- Zheng, Y., Olson, M., Hall, A., Cerione, R., & Toksoz, D. (1995) *J. Biol. Chem.* 270(16), 9031–9034.

BI9622837